Monatshefte für Chemie 134, 1529–1539 (2003)
DOI 10.1007/s00706-003-0077-2

Monatshefte für Chemie
Chemical Monthly
Printed in Austria

The Effect of Alkane Chain Length on the Liquid–Liquid Critical Temperatures of Oligostyrene/Linear-Alkane Mixtures

Attila R. Imre[1,*], **W. Alexander Van Hook**[2], **Bong Ho Chang**[3], and **Young Chan Bae**[3]

[1] KFKI Atomic Energy Research Institute, POB 49, H-1525 Budapest, Hungary
[2] Chemistry Department, University of Tennessee, Knoxville, TN 37996-1600, USA
[3] Division of Chemical Engineering, Hanyang University, Seoul 133-791, Korea

Received April 30, 2003; accepted (revised) June 22, 2003
Published online October 6, 2003 © Springer-Verlag 2003

Summary. Upper critical solution temperatures (UCSTs) for liquid–liquid demixing in a set of mixtures of linear alkanes (pentane (N_1=5) to pentacontane (N_1=50)) with an oligostyrene (1241 amu, N_2=12) are reported. We find strong correlation between the *Hildebrand* solubility parameters of the alkanes and the UCST. Correlations are developed which enable predictions concerning the miscibility of mixtures of compounds with longer chains.

Keywords. Polystyrene; Alkanes; UCST; Miscibility; Liquid–liquid equilibrium; Solubility parameter.

Introduction

The system polyethylene (more generally, polyolefins) and polystyrene is commonly referred to as the classical example of an incompatible (immiscible) polymer pair. This immiscibility is unfortunate because it complicates the recycle technology of these abundant and very common materials. While it is well established that homogeneous blending of polyolefin/polystyrene is impossible at ordinary conditions for polymers of significant chain length, it is interesting to explore the limits of miscibility in (T, P, N_1, N_2) space (T is temperature, P pressure, N_1 polyolefin segment number, and N_2 polystyrene segment number). As it is impossible to carry out liquid–liquid phase equilibrium measurements in polyethylene/polystyrene mixtures, information on miscibility limits can only be obtained

* Corresponding author. E-mail: imre@sunserr.kfki.hu

indirectly, for example from demixing studies of polymers and common solvents or by inverse gas chromatography [1–3]. An alternative approach is via studies of liquid–liquid equilibria in oligomer systems, and to that end we have systematically studied demixing equilibria of oligostyrene/oligoethylene and polystyrene/oligoethylene systems, and reported the effects of branching [4], pressure [5], and end-group [6] on miscibility. In this paper we extend these studies and report new experimental results on the effect of alkyl-chain length on the miscibility of mixtures of a fixed length oligostyrene (1241 amu, N_2=12) with variable length *n*-alkanes (from N_1=5 to 50, as oligoethylenes). Although it is well known that miscibility decreases with chain length, quantification of the magnitude of the decrease and the definition of the limits of partial miscibility still require experimental study.

Results and Discussion

Phenomenological Description

Cloud points are listed in Table 1 and plotted in Fig. 1. The cloud point curves (CPCs) exhibit UCST behaviour. For strictly binary systems the maximum (T_{max}) corresponds exactly to the UCST, while for systems of small polydispersity T_{max} approximates UCST within present experimental precision [7]. At higher polydispersity, CPCs distort, in some cases even developing double maxima [7–9], where UCST approximately corresponds to T at the (local) minimum. In the present study polydispersity of the oligostyrene and the lower alkanes is small, but for oligostyrene/alkane mixtures (N_1=40 and 50) local minima in CPC are observed which we ascribe to alkane polydispersity. Accordingly, for mixtures with N_1=5 to 30 UCST=T_c was taken as T_{max}, while for N_1=40 and 50, where CPC shows double maxima and a local minimum (Table 1, Fig. 1), we set T_c=$T_{local\ min}$ (see for example [8]). UCSTs (T_cs) are listed in Table 2 and plotted in Fig. 2, where they are compared with literature values for related systems [10, 11].

It is well established that weakly interacting polymeric mixtures exhibit demixing curves with upper and lower consolute branches (UCS and LCS), with UCST<LCST (*i.e.* $T_c(UCS) < T_c(LCS)$) (Fig. 2a). In some systems, as chain length increases, the branches merge to form an hourglass-shaped phase diagram. Generally, for such systems, UCST increases and LCST decreases with increasing chain length [7, 12], but this is not true in the present case. For oligostyrene/alkane mixtures (N_1 small) UCST initially decreases with increasing N_1 [11], and then increases after passing through an N_2-dependent minimum (Fig. 2b). A review of literature data [10] reveals that LCST initially increases with N_1. We do not have data for LCST at higher N_1s, but expect that after passing a local maximum it will decrease as it does for the other weakly interacting polymeric mixtures [7, 12].

The homogeneous region for the systems of present interest (*i.e.* that part of the diagram lying between the UCS and LCS branches) is found inside a leaf-shaped region between the freezing and liquid–vapour critical temperatures of the pure alkanes (Fig. 2a, b). At small enough N_1, UCST and LCST move toward each other as N_1 increases and eventually meet, thereby defining a double critical point (an extremum on the critical line) like the one marked in the diagram (Fig. 2) as

Table 1. Cloud point temperatures of the studied oligostyrene/*n*-alkane systems

n-pentane[a] $N_1=5$		*n*-hexane[a] $N_1=6$		*n*-heptane $N_1=7$		*n*-octane[a] $N_1=8$	
100 w	T_{cp}/K	100 w	T_{cp}/K	100 w	T_{cp}/K	100 w	T_{cp}/K
10.0	281.0 ± 0.2	6.3	263.2 ± 0.5	10.0	269.2 ± 0.3	10.0	271.5 ± 0.2
13.0	283.1 ± 0.2	8.3	267.4 ± 0.2	13.0	272.0 ± 0.2	13.0	273.5 ± 0.2
16.0	284.9 ± 0.2	12.3	271.2 ± 0.2	16.0	273.7 ± 0.2	16.0	275.7 ± 0.2
19.0	283.4 ± 0.3	16.2	274.6 ± 0.2	19.0	274.9 ± 0.2	19.0	277.2 ± 0.2
20.3	285.0 ± 0.1	17.6	274.9 ± 0.2	22.0	275.4 ± 0.2	22.0	278.0 ± 0.2
21.4	283.8 ± 0.3	19.2	274.7 ± 0.2	25.9	275.5 ± 0.2	25.0	278.2 ± 0.2
22.9	285.4 ± 0.2	21.9	274.4 ± 0.2	33.7	274.4 ± 0.2	28.5	278.2 ± 0.2
23.4	285.7 ± 0.2	24.3	273.8 ± 0.2			35.0	277.3 ± 0.2
24.8	285.5 ± 0.1						
27.0	285.6 ± 0.2						
29.8	285.5 ± 0.1						
32.7	284.8 ± 0.2						

n-decane $N_1=10$		*n*-dodecane $N_1=12$		*n*-tetradecane $N_1=14$		*n*-octadecane $N_1=18$	
100 w	T_{cp}/K	100 w	T_{cp}/K	100 w	T_{cp}/K	100 w	T_{cp}/K
10.0	277.1 ± 0.2	10.0	286.2 ± 0.2	15.0	301.7 ± 0.3	29.1	320.8 ± 0.2
13.0	280.3 ± 0.2	15.0	292.3 ± 0.2	20.0	302.6 ± 0.2	44.6	320.7 ± 1.0
16.0	282.4 ± 0.2	20.0	293.4 ± 0.3	25.0	304.0 ± 0.2	51.8	320.7 ± 0.5
19.0	283.7 ± 0.2	25.0	294.6 ± 0.2	30.0	304.0 ± 0.2	57.1	319.7 ± 1.5
22.0	284.7 ± 0.2	30.0	294.9 ± 0.2	35.0	303.8 ± 0.2	62.9	314.2 ± 1.0
25.0	285.1 ± 0.2	35.0	295.0 ± 0.2	40.0	303.6 ± 0.2	65.0	315.4 ± 0.5
28.0	285.1 ± 0.2	40.0	294.1 ± 0.1	40.0	303.5 ± 0.2	72.7	312.7 ± 1.5
31.0	285.0 ± 0.2	45.0	293.7 ± 0.2	45.0	303.0 ± 0.3		
35.4	284.8 ± 0.1	48.4	292.8 ± 0.2	47.6	301.9 ± 0.3		
				49.6	302.9 ± 0.3		

n-triacontane $N_1=30$		*n*-tetracontane $N_1=40$		*n*-pentacontane $N_1=50$	
100 w	T_{cp}/K	100 w	T_{cp}/K	100 w	T_{cp}/K
44.5	365.7 ± 0.5	41.0	386.7 ± 0.3	39.7	395.4 ± 0.5
55.5	364.2 ± 0.5	44.9	387.2 ± 0.3	45.7	407.2 ± 0.1
62.2	363.7 ± 0.5	47.9	385.7 ± 0.3	50.3	401.8 ± 0.1
66.9	362.7 ± 0.5	50.4	385.2 ± 0.3	58.5	405.5 ± 0.3
		56.5	386.7 ± 0.3	64.5	399.2 ± 0.3
		59.3	387.2 ± 0.3		
		68.9	387.2 ± 0.3		

[a] From Ref. [4]

$N_{1\text{-}cmin}$. For $N_1 < N_{1\text{-}cmin}$ the components exhibit hourglass-shaped miscibility diagrams [7]. The precise value of $N_{1\text{-}cmin}$ and its corresponding double critical temperature, T_{dcp} depends on the molar mass (or chain length N_2) of the oligostyrene;

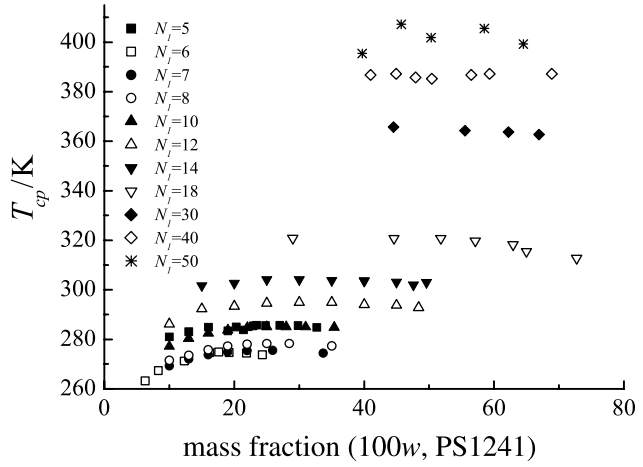

Fig. 1. Cloud point curves (T_{cp}) of mixtures of oligostyrene (1241 *amu*) with *n*-alkanes, from pentane (N_1=5) to pentacontane (N_1=50)

Table 2. *Hildebrand* solubility parameters and molar volumes for the studied *n*-alkanes, together with the experimental and calculated UCSTs for their mixture with the studied oligostyrene (1241 *amu*)

Component	N_1	δ_{ALK}/MPa$^{1/2}$ (at 298 K)	V_{ALK}/cm^3 mol^{-1} (at 298 K)	UCST/K (experimental)	UCST/K (by Eq. (1))
n-pentane	5	14.5	115.2	285.7±0.2	272.4
n-hexane	6	14.9	130.5	274.9±0.2	267.4
n-heptane	7	15.3	146.6	275.5±0.2	271.1
n-octane	8	15.6	162.5	278.2±0.2	278.6
n-decane	10	15.8	194.9	285.1±0.2	299.9
n-dodecane	12	16.0	227.5	295.0±0.2	324.4
n-tetradecane	14	16.2±0.1[a]	260.1	304.0±0.3	350±5
n-octadecane	18	16.4±0.1[a]	327.6	321±1	401±5
n-triacontane	30	16.7±0.1[a]	545.6	363±1	545±5
n-tetracontane	40	16.8±0.1[a]	742±1[b]	385±1	650±5
n-pentacontane	50	16.9±0.1[a]	954±1[b]	402±2	746±5

[a] From linear interpolation ($1/N_1$ *vs.* δ_{ALK}) of the lower alkanes; [b] From quadratic extrapolation ($\log(1/N_1)$ *vs.* $\log V_{ALK}$) of lower alkanes

for PS4000 ($N_{1\text{-}cmin}$, T_{dcp}) ~ (6, 390 K), for PS2030 ($N_{1\text{-}cmin}$, T_{dcp}) ~ (5, 360 K), and for PS1241 it is expected ($N_{1\text{-}cmin}$, T_{dcp}) ~ (4, 325 K). For $N_1 > N_{1\text{-}cmin}$ the miscibility gap lying between UCST and LCST might possibly continue to increase with N_1 (*i.e.* LCST will increase with increasing chain-length), but this is unlikely for entropic reasons [7]. More probably the LCST will go through a maximum as N_1 continues to increase, beyond which the miscibility gap will shrink and eventually UCST and LCST will join again, this time at a second N_2-dependent double critical point, $N_{1\text{-}cmax}$, provided thermal degradation has not yet occurred.

Based on our analysis of the data in Fig. 2 we propose a distinction between two types of incompatibility for solutions of oligostyrenes (and eventually polystyrene)

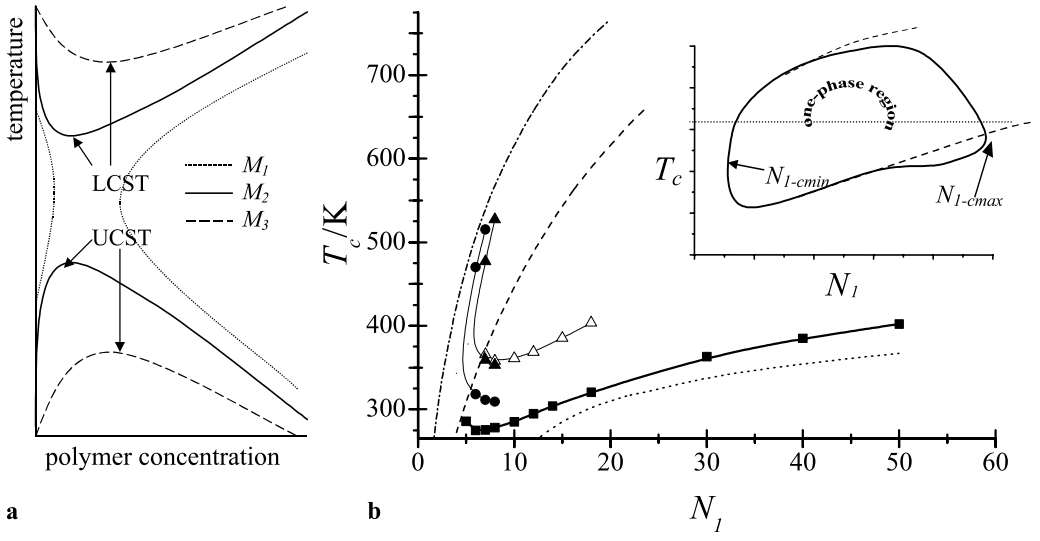

Fig. 2. a. Schematic representation for the liquid–liquid phase equilibrium in a weakly interacting binary polymeric system (solution or blend) showing two separated solubility branches; with increasing the chain length of one component, the two branches move closer together, and in some cases the branches merge and form hourglass-shaped demixing diagrams [7]; b. Liquid–liquid critical temperatures (UCSTs and LCSTs) for different oligostyrene-*n*-alkane mixtures; closed squares: UCSTs for PS1241/*n*-alkane mixtures (this paper), open triangles: UCSTs for PS4000/*n*-alkanes (from Ref. [11]), circles: UCSTs and LCSTs for PS2030/*n*-alkane mixtures (from Ref. [10]), full triangles: UCSTs and LCSTs for PS4800 (from Ref. [10]), connecting solid lines serve only as guide for the eye; liquid–vapour critical temperatures, boiling temperatures (at atmospheric pressure), and melting temperatures for the pure *n*-alkanes are plotted with dash-dotted, dashed, and dotted lines, respectively; Insert: Schematic representation for two different scenarios to be ''incompatible''; solid line: real incompatibility (no miscibility above a certain N_1), the one-phase region is an island, dashed line: virtual incompatibility, the line of compatibility (the UCST) moves above the degradation temperature (dotted line) as N_1 approaches high values; $N_{1\text{-}cmin}$ and $N_{1\text{-}cmax}$ mark the two limiting chain length (see text)

with higher mass alkanes (and eventually polyethylene), see Fig. 2b and insert, by considering the N_2 dependence of ($N_{1\text{-}cmin}$, T_{dcp}). First, as N_2 increases so does ($N_{1\text{-}cmin}$, T_{dcp}), and T_{dcp} eventually increases to the point where it exceeds the degradation temperature of the polymers. For polystyrene this temperature is around 600 K while for polyethylene it is in the range 571–723 K [13]. Thus, for N_2 greater or equal to this value, and N_1 greater or equal to $N_{1\text{-}cmin}$, the mixtures cannot be homogenized (except at very low mass fraction, *w*, hour-glass configuration). We label this case ''real incompatibility''. This limiting value of N_1 is a double critical point ($N_{1\text{-}cmax}$). The second case (represented by the dashed line in the insert) is found when separate UCST and LCST exist even for high M_w (with, as usual, a homogeneous region between them), but the lower branch (the UCST) has moved above the degradation temperature (dotted line) for long chains. In this case, although the polymers would be compatible (if they had not decomposed), it is impossible to reach the temperature necessary for their homogenization. We label this ''virtual incompatibility''.

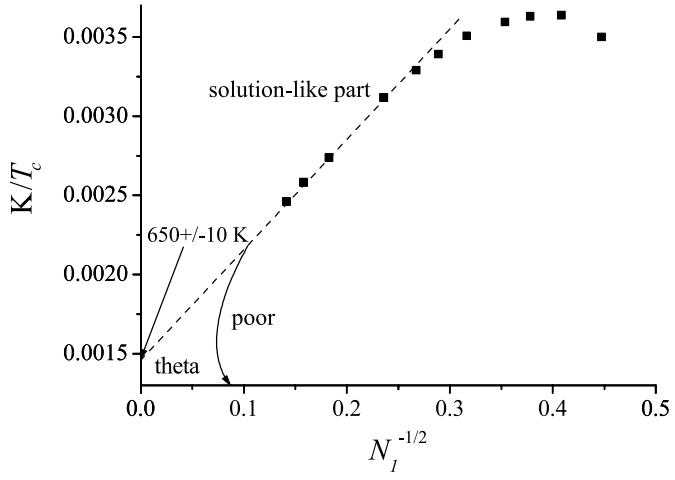

Fig. 3. *Shultz-Flory* plot for PS1241/*n*-alkane mixtures; above N_1=14 the dependence ($N_1^{-1/2}$ *vs.* $1/T_c$) is linear (dashed line, K/T_c=0.00148(±0.00002)+0.0069(±0.0001)×$N_1^{-1/2}$, R^2= 0.9998); real incompatibility (see Fig. 1) is represented by a solid arrow (PS1241 behaves as poor solvent for polyethylenes), virtual incompatability is represented by the extension of the dashed line (theta behaviour with Θ=650±10 K)

Classical *Flory* theory [14] predicts a linear dependence between $N^{-1/2}$ and $1/T_c$ for solutions and this has been verified down to N=7 for polystyrene solutions in common small molecule solvents [12, 15]. Also, *Flory* theory predicts a linear N-dependence for UCST in polymer blends. For the present systems neither one of these predictions seems to be correct. The chain-length dependences of UCST in alkyl chain-molecule + oligo- or polystyrene mixtures may exhibit minima [11], as it is seen for the present data (Fig. 2b), and previously explained in terms of endgroup effects [6, 16]. Figure 3 is a *Shultz-Flory* plot ($N_1^{-1/2}$ *vs.* $1/T_c$) of the present data and shows good linearity in the region N_1=14 to N_1=50, *i.e.* over that range of N_1 the system behaves like a polymer solution (with the 12-unit oligostyrene as solvent). When the *Shultz-Flory* function is extrapolated to infinite chain length one estimates a theta temperature (650±10 K) for the polyethylene/PS1241 system, somewhat higher than the degradation temperatures of PS (~600 K) and PE (~570 K). Obviously this extrapolation holds only true if the solution is virtually incompatible (scenario two (Fig. 2b, insert, dashed line)); if it showed real incompatibility one would expect the curve to turn back showing typical poor-solvent behaviour [12]. For long-chain-PE/long-chain-PS systems one expects that the critical temperatures (if there are any) will lie well above the degradation temperature of the polymers.

Correlations

For some binary systems UCSTs can be reasonably correlated with the molar volumes of the component of variable chain length [17]. Molar volume for PS was calculated from its M_w (1241 amu) and density (1.05 g/cm^3) as 1181 cm^3/mol. Molar volumes for alkanes (up to N_1=30) were obtained from standard references

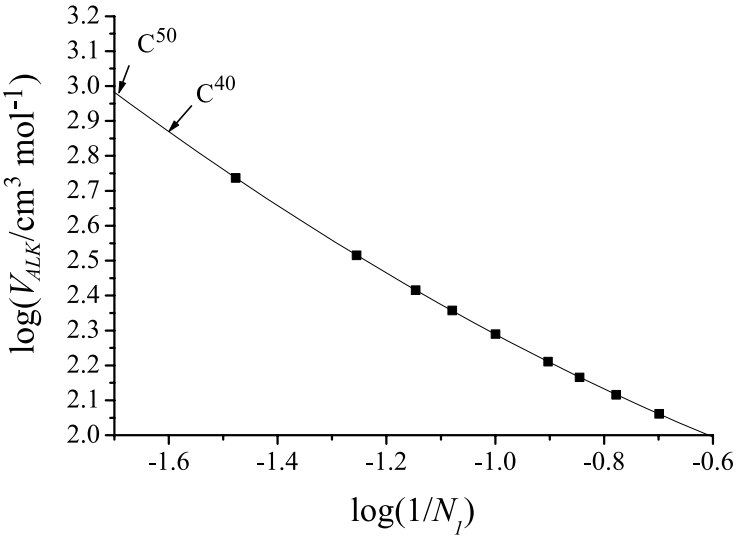

Fig. 4. Extrapolation of literature values for *n*-alkane molar volumes (C^5 to C^{30}) to C^{40} and C^{50}; ($\log(V_{ALK}/\mathrm{cm}^3\ \mathrm{mol}^{-1})=1.690(\pm0.005)-0.370(\pm0.009)\times\log(1/N_1)+0.229(\pm0.004)\times\log^2(1/N_1)$, $R^2=0.99999$); predicted molar volumes for tetracontane and pentacontane are marked by arrows

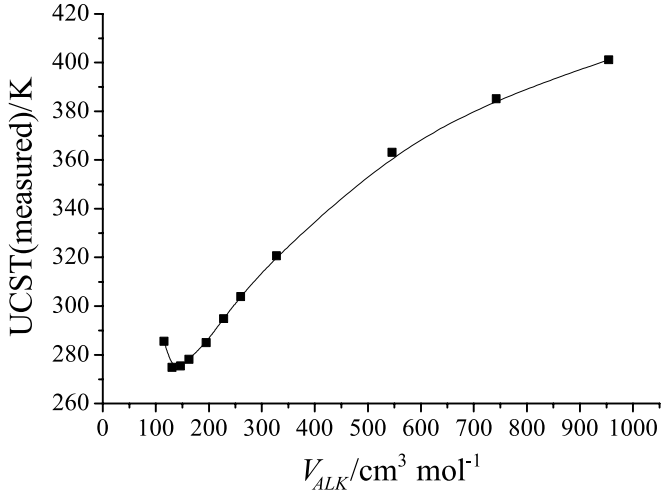

Fig. 5. Correlation of the measured UCSTs with the molar volumes of the alkanes; the solid line serves as a guide for the eye

[18], and those for $N_1=40$ and $N_1=50$ by extrapolation (Fig. 4). Figure 5 demonstrates a correlation between UCST and V, the minimum near $N_1=7$ is ascribed to endgroup (methyl) effects. A similar correlation attempted for (oligostyrene+branched and/or cyclic alkane) systems was less successful [4].

Correlations of miscibility with *Hildebrand* or *Hansen* solubility parameters are well established [19–21]. A long established rule-of-thumb maintains that for miscibility the *Hildebrand* parameters should be nearly equal [21–23], but this,

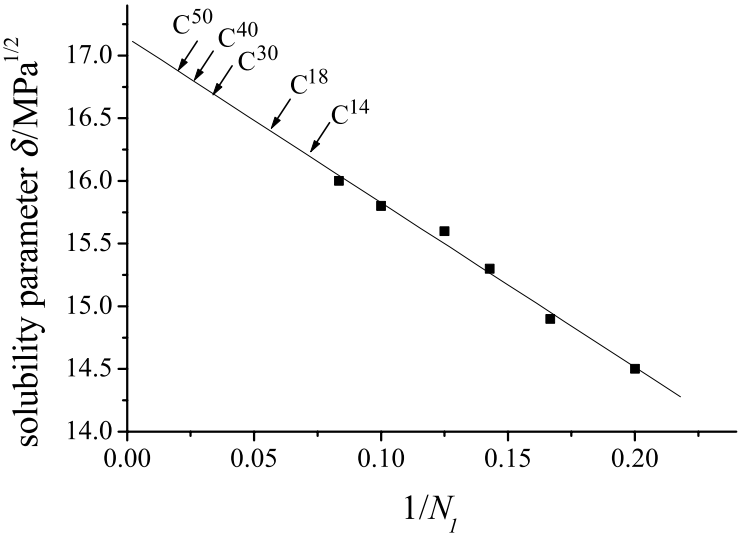

Fig. 6. Extrapolation of *Hansen* solubility parameters (C^5 to C^{12}) to C^{50} ($\delta_{ALK}/MPa^{1/2}=17.14(\pm0.10)-13.1(\pm0.7)\times 1/N_1$, $R^2=0.995$); expected values for C^{14} to C^{50} are marked by arrows

unfortunately, is an oversimplification as there are many, many exceptions [12]. The situation improves with the use of the more complex *Hansen* solubility approach [12, 21] which includes both polar and nonpolar terms. The present systems combine a typically apolar component (alkane) with a slightly polar one (polystyrene). *Hildebrand* solubility parameters for the alkanes are quoted in Table 2; for apolar compounds the *Hildebrand* parameter is equal to the apolar part of the *Hansen* parameter. For polystyrene previously used values are $\delta_{d\text{-}PS}=16.8\,MPa^{1/2}$ and $\delta_{p\text{-}PS}=7.5\,MPa^{1/2}$ [4], and the recommended value for the *Hildebrand* parameter is 18.5 [21]. Alkane solubility parameters (δ_{ALK}) for $N_1\leq 12$ were taken from Ref. [19]; and those for $N_1\geq 14$ obtained by extrapolation (Fig. 6). That this is reasonable is established by comparing the $1/N_1=0$ value, $17.2\,MPa^{1/2}$, with the preferred value for long-chain polyethylene, $17.0\,MPa^{1/2}$ [19]; the agreement is good. In any event the resulting correlation, which is smooth and well behaved (Fig. 7), is well described by a fourth-order polynomial.

The *Weimer-Prausnitz* version of regular solution theory [24, 25] has previously been applied to demixing of acetonitrile-alkane [26], butanenitrile-alkane [27] and oligostyrene-short branched and cyclic alkane [4] solutions with success. According to this theory, UCSTs of solutions of polystyrene in nonpolar, nonhydrogen bonded solvents can be calculated using Eq. (1).

$$\mathrm{UCST} = 2\left[\frac{(\delta_{d\text{-}PS}-\delta_{ALK})^2+\delta_{p\text{-}PS}^2-2\Psi_{PS\text{-}ALK}}{R}\right]\left[\frac{V_{PS}V_{ALK}}{(V_{PS}^{1/2}+V_{ALK}^{1/2})^2}\right] \qquad (1)$$

Here $\delta_{d\text{-}PS}$ is the nonpolar (dispersive) part of the total solubility parameter for the polar component (PS), $\delta_{p\text{-}PS}$ is the polar part of the solubility parameter of the polar component, δ_{ALK} is the solubility parameter of the nonpolar component, V_{PS} and V_{ALK} are molar volumes for the PS and the alkane, R is the gas constant,

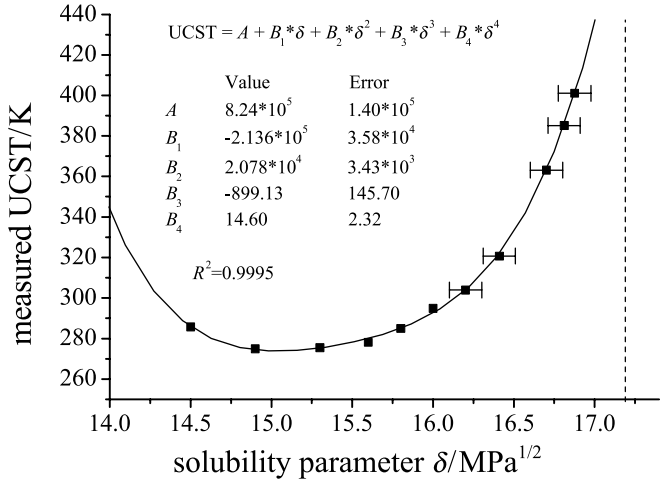

Fig. 7. Correlation of measured UCSTs with *Hansen* solubility parameters of the alkanes, fitting parameters are reported in the insert; dashed line represents the extrapolated solubility parameters for infinite chain-length polyethylene

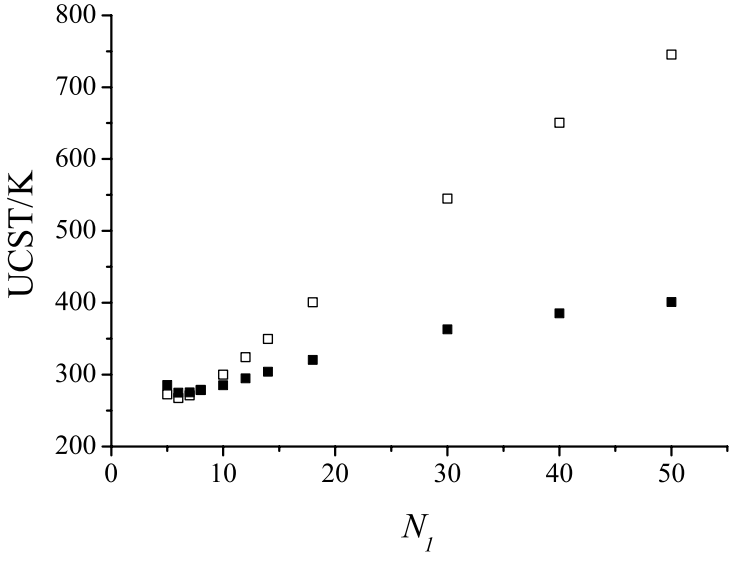

Fig. 8. Comparison of the calculated UCSTs (by Eq. (1)) with experimental data; open squares: calculated UCSTs, full squares: measured UCSTs

and $\Psi_{PS\text{-}ALK}$ is the induction energy density. For hydrocarbons $\Psi_{PS\text{-}ALK}=0.396\delta_\tau^2$ [24].

For the calculations, solubility parameters and molar volumes (Table 2) obtained at 298 K were used. Calculated UCSTs are compared with experimental data in Table 2 and Fig. 8. Although the theory verified the existence of the minimum in N_1 *vs.* T_c, agreement between calculation and experiment fails badly for $N_1>\sim 15$ (Fig. 8).

Summary

Cloud point curves and liquid–liquid critical temperatures have been presented for a series of mixtures of an 12-unit oligostyrene (1241 *amu*) with linear alkanes (pentane (N_1=5) to pentacontane (N_1=50)). The chain-length dependence of UCSTs shows a minimum, which is ascribed to an endgroup effect. The UCSTs are well correlated with the *Hildebrand* solubility parameters of the alkanes. The *Weimer-Prausnitz* version of regular solution theory, previously applied with success to several different series of alkane-containing mixtures, was not able to describe the present results quantitatively. The analysis of trends in the phase diagrams generated in this work permits qualitative predictions concerning miscibility of mixtures of longer chain molecules (polyethylene and polystyrene).

Experimental

List of Symbols

T_{cp} cloud point temperature; T_{max} temperature corresponding to the maximum of the cloud point curve; T_c liquid–liquid critical temperature; w mass fraction; UCST upper critical solution temperature; LCST lower critical solution temperature; N segment number in general; N_1 number of carbon atoms in the alkanes (segment number); N_2 polystyrene segment number; $N_{1\text{-}cmin}$ critical (minimum) alkane segment number; $N_{1\text{-}cmax}$ critical (maximum) alkane segment number; M_w weight-average molecular weight; M_n number average molecular weight; $\delta_{d\text{-}PS}$ nonpolar part of the solubility parameter (PS); $\delta_{p\text{-}PS}$ polar part of the solubility parameter (PS); δ_{ALK}, δ_{PS} *Hildebrandt* solubility parameter (alkanes and polystyrene); V_{PS}, V_{ALK} molar volumes for PS and alkanes; $\Psi_{PS\text{-}ALK}$ induction energy density; Θ theta temperature.

Materials

Polystyrene (PS1241, M_w=1.241 kg/mol, M_w/M_n=1.07) was obtained from Pressure Chemical Co. Research grade linear alkanes from pentane (C^5) to pentacontane (C^{50}) were obtained from Aldrich Chemical Co. All substances were used as received.

Apparatus and Sample Preparation

Mixtures were prepared gravimetrically and loaded into thin-wall glass capillaries, containing small steel mixing bars. Capillary tubes were closed by flame or by teflon plug and samples were homogenized by continuous mixing at least 10 K above their cloud point temperature. Liquid–liquid equilibrium (cloud point) curves were measured by visual determination of the temperature of onset of turbidity when gradually decreasing T (0.1 K steps, waiting several minutes at each step for equilibrium). Cloud point temperatures were determined with a reproducibility of 0.1–0.5 K.

Acknowledgements

This work was supported by a US Department of Energy grant, the *Ziegler* Research Fund of the Chemistry Department, University of Tennessee, by the Hungarian Research Fund OTKA (T043042), and by a bilateral grant between the Korean Science and Engineering Foundation and the Hungarian Academy of Science. One of the authors (*A.R.I.*) was supported also by a Bolyai Research Fellowship.

References

[1] Bonifaci L, Ravanetti GP (1993) J Chromatography **641**: 301–307
[2] Bogilo VI, Voelkel A (1995) J Chromatogr A **715**: 127–134
[3] Petri H-M, Horst R, Wolf BA (1996) Polymer **37**: 2709–2713
[4] Imre AR, Van Hook WA (2001) Fluid Phase Eq **187–188**: 363–372
[5] Imre AR, Melnichenko G, Van Hook WA, Wolf BA (2001) Phys Chem Chem Phys **3**: 1063–1066
[6] Imre AR, Van Hook WA (2000) Macromolecules **33**: 5308–5309
[7] Koningsveld R, Stockmayer WH, Nies E (2001) Polymer Phase Diagrams. Oxford University Press, New York
[8] Koningsveld R, Onclin MH, Kleintjens LA (1982) In: Solc K (ed) Polymer compatibility and incompatibility, Principles and Practices, MMI Press Symposium Series, vol 2, Harwood Academic Publisher Chur, p 25
[9] Solc K, Stockmayer WH, Lipson JEG, Koningsveld R (1989) In: Culbertson BM (ed) Multiphase Macromolecular Systems. Plenum Publishing Corp
[10] Cowie JMG, McEwen IJ (1983) Polymer **24**: 1445–1448
[11] van Opstal L, Koningsveld R, Kleintjens LA (1991) Macromolecules **24**: 161–167
[12] Imre A, Van Hook WA (1996) J Phys Chem Ref Data **25**: 637–661 (Erratum: 25 (1996) 1277)
[13] van Krevelen DW (1997) Properties of Polymers, 3rd ed, chapt 21, Elsevier, Amsterdam
[14] Flory PJ (1953) Principles of Polymer Chemistry. Cornell Univ Press, Ithaca
[15] Imre A, Van Hook WA (1996) J Polym Sci B **34**: 751–760
[16] Schuch W, Wolf BA (1981) Makromol Chem **182**: 1801–1818
[17] Eustaquio-Rincón R, Ascención R-M, Trejo A (1993) Fluid Phase Eq **91**: 187–201
[18] Lide DR (ed) (1990) CRC Handbook of Chemistry and Physics, 71st ed, CRC Press, Boca Raton
[19] Grulke EA (1989) In: Brandrup J, Immergut EH (eds) Polymer Handbook, 3rd ed, chapt VII, John Wiley & Sons, pp 519–559
[20] Barton AFM (1990) CRC Handbook of Polymer-Liquid Interaction Parameters and Solubility Parameters. CRC Press, Boca Raton
[21] Barton AFM (1991) CRC Handbook of Solubility Parameters and Other Cohesion Parameters. CRC Press, Boca Raton
[22] Chen SA (1971) J Appl Polym Sci **15**: 1247–1266
[23] Seymour RB (1982) In: Seymour RB, Stahl GA (eds) Macromolecular Solutions. Pergamon Press, New York, pp 10–13
[24] Weimer RF, Prausnitz JM (1965) Hydrocarbon Process **44**: 237–242
[25] Hildebrand JH, Prausnitz JM, Scott RL (1970) Regular and Related Solutions, the Solubility of Gases, Liquids and Solids. Van Nostrand-Reinhold, New York
[26] Cuevas RM, Eustaquio-Rincón R, Ascención R-M, Trejo A (1995) Fluid Phase Eq **107**: 201–212
[27] Eustaquio-Rincón R, Ramírez LF, Trejo A (1998) Fluid Phase Eq **149**: 177–189